

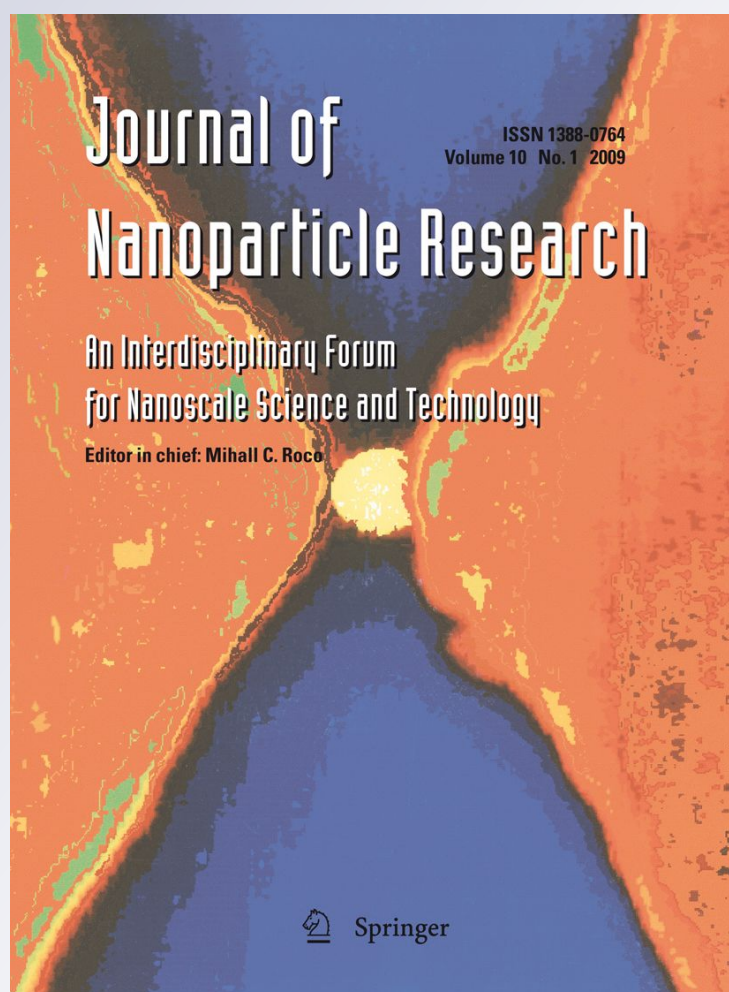
Microwave-assisted hydrothermal synthesis of biocompatible silver sulfide nanoworms

Ruimin Xing, Shanhu Liu & Shufang Tian

Journal of Nanoparticle Research
An Interdisciplinary Forum for
Nanoscale Science and Technology

ISSN 1388-0764
Volume 13
Number 10

J Nanopart Res (2011) 13:4847-4854
DOI 10.1007/s11051-011-0462-4



 Springer

Your article is protected by copyright and all rights are held exclusively by Springer Science+Business Media B.V.. This e-offprint is for personal use only and shall not be self-archived in electronic repositories. If you wish to self-archive your work, please use the accepted author's version for posting to your own website or your institution's repository. You may further deposit the accepted author's version on a funder's repository at a funder's request, provided it is not made publicly available until 12 months after publication.

Microwave-assisted hydrothermal synthesis of biocompatible silver sulfide nanoworms

Ruimin Xing · Shanhu Liu · Shufang Tian

Received: 23 November 2010 / Accepted: 9 June 2011 / Published online: 23 June 2011
© Springer Science+Business Media B.V. 2011

Abstract In this study, silver sulfide nanoworms were prepared via a rapid microwave-assisted hydrothermal method by reacting silver nitrate and thioacetamide in the aqueous solution of the Bovine Serum Albumin (BSA) protein. The morphology, composition, and crystallinity of the nanoworms were characterized by field emission scanning electron microscopy (FESEM), X-ray powder diffraction (XRD), transmission electron microscopy (TEM), selected area electron diffraction (SAED), X-ray energy dispersive spectroscopy (EDS), and Fourier transform infrared (FTIR) spectroscopy. The results show that the nanoworms were assembled by multiple adjacent Ag_2S nanoparticles and stabilized by a layer of BSA attached to their surface. The nanoworms have the sizes of about 50 nm in diameter and hundreds of nanometers in length. The analyses of high-resolution TEM and their correlative Fast Fourier Transform (FFT) indicate that the adjacent Ag_2S

nanoparticles grow by misoriented attachment at the connective interfaces to form the nanoworm structure. In vitro assays on the human cervical cancer cell line HeLa show that the nanoworms exhibit good biocompatibility due to the presence of BSA coating. This combination of features makes the nanoworms attractive and promising building blocks for advanced materials and devices.

Keywords Microwave · Silver sulfide · Nanoworms · Biocompatibility · Protein coating

Introduction

During the past few decades, semiconductor nanomaterials have been of great interest because of their optical and electrical properties, which may be widely used in the area of optoelectronics or bioapplications. Among all these semiconductors, chalcogenide semiconductor nanocrystals (metal sulfides and selenides) have attracted broad attention because of their unique shape- and size-dependent physical and chemical properties that differ drastically from their bulk counterparts (Mao et al. 2010; Qin et al. 2008; Teranishi et al. 2009; Wang et al. 2009). Therefore, chalcogenide semiconductor nanocrystals have been extensively pursued from material scientists and information-recording specialists due to the unique possibility of optical imaging and optical information

R. Xing · S. Liu (✉) · S. Tian
Institute of Molecular and Crystal Engineering, College of Chemistry and Chemical Engineering, Henan University, Kaifeng 475001, People's Republic of China
e-mail: liushanhu@163.com; shanhuliu@henu.edu.cn

R. Xing
e-mail: rxming@henu.edu.cn

R. Xing
State Key Laboratory of Coordination Chemistry, School of Chemistry and Chemical Engineering, Nanjing University, Nanjing, People's Republic of China

storage (Du et al. 2010; Sadtler et al. 2009). As a chalcogenide semiconductor with a direct band gap of ~ 1.0 eV at room temperature and relatively high absorption coefficient ($10^4 \text{ M}^{-1} \text{ cm}^{-1}$), monoclinic α - Ag_2S has a variety of potential applications, such as photoconductors, photovoltaic cells, solar-selective coating, near-IR bioimaging, and biosensing (Liao et al. 2009; Pan et al. 2007; Xu et al. 2010; Yang et al. 2006; Zhang et al. 2000).

Being promising materials with potential applications, many efforts have been focused on the synthesis and fabrication of Ag_2S nanomaterials to enhance its performance in currently used applications in photography and luminescent devices (Brelle et al. 1999; Choi et al. 2009; Lim et al. 2004; Liu et al. 2002, 2004). Silver sulfide nanowire arrays were synthesized by anodic aluminum oxide template and by a gas–solid reaction approach (Jang et al. 2007; Niu et al. 2007). Self-supported pattern of Ag_2S nanorod arrays was created by a solution-growth method (Lu et al. 2002). Highly ordered Ag_2S nanorods were fabricated at ambient temperature via a biomimetic strategy (Yang et al. 2006). Silver-based nanofiber bundles were synthesized with $\text{Ag}_2\text{C}_2\text{O}_4$ nanofiber bundles as a general sacrificial template (Wang and Qi 2008). However, there still remains a great challenge to develop a simple and rapid synthetic route to prepare Ag_2S nanostructures with highly controlled dimensions, morphology, phase purity, and chemical composition because of the complexity in the chemical behavior of these materials (Wang et al. 2008).

In this study, a rapid microwave-assisted hydrothermal method was developed for the facile synthesis of silver sulfide nanoworms in the BSA aqueous solution. BSA was used as stabilizer, since it has a strong affinity to a variety of inorganic molecules binding to different sites, which makes possible the utilization of BSA-decorated nanomaterials in a variety of supramolecular assemblies (Mamedova et al. 2001). Microwave-assisted hydrothermal method was chosen as the efficient, inexpensive, and green heating style with reaction times reduced to order of minutes (Liu et al. 2011a, b). Moreover, microwave irradiation offers rapid and uniform heating in solution relative to conventional heating and thus provides more homogeneous nucleation and shorter crystallization time, which is greatly advantageous for the preparation of nanomaterials (Baruwati et al. 2009; Pal et al. 2009; Pastoriza-Santos and Liz-Marzán 2002; Song et al.

2010; Wu et al. 2010; Zhu et al. 2000, 2004). To the best of our knowledge, this is the first report of microwave-assisted hydrothermal synthesis of silver sulfide nanoworms. Microstructural analyses reveal that the nanoworms were assembled by the misoriented attachment of multiple adjacent Ag_2S nanoparticles and stabilized by a layer of BSA. Furthermore, the potential cellular toxicity of the nanoworms was evaluated on HeLa cells by 3-(4,5-dimethylthiazol-2-yl)-2,5-diphenyltetrazolium bromide (MTT) assay.

Experimental section

Materials

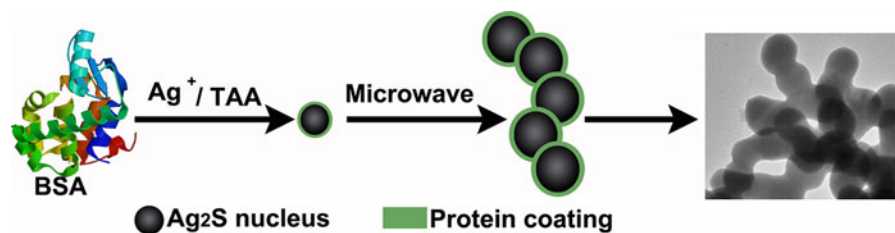
BSA (Purity $\geq 98\%$, Mw = 68,000) was purchased from Sigma-Aldrich. Silver nitrate ($\geq 99.8\%$) and thioacetamide (TAA, $\geq 99.0\%$) and other chemical reagents were of analytic grade and used as received without further purification. Millipore water ($18.2 \text{ M}\Omega \cdot \text{cm}$ at 25°C) was used throughout all the experiments.

Fabrication of the Ag_2S nanoworms

In a typical process, 10 mL of 50 mM silver nitrate aqueous solution and 20 mL of 1 mg/mL BSA aqueous solution were mixed with vigorous stirring at room temperature. The mixed solution of the BSA– Ag^+ emulsion was kept static under nitrogen protection for 6 h. Then 10 mL of 50 mM TAA aqueous solution was added. Immediately after TAA addition, the solution changed to black, indicating the formation of colloidal Ag_2S nuclei. Then 40 mL of the solution was sealed in autoclaves (80-mL capacity) and irradiated to 200°C for 50 min. The black solid products were collected and washed at least three times with water and ethanol, and then dried under vacuum at room temperature.

Cytotoxicity assay

Growth inhibitory effect of the BSA– Ag_2S nanoworms on HeLa cells was tested by the MTT assay (Xing et al. 2009b). In Brief, HeLa cells were grown in Dulbecco's modified Eagle's medium (DMEM, Gibco) supplemented with fetal bovine serum (10%, v/v), streptomycin (0.1 mg mL^{-1}), and penicillin



Scheme 1 The route to fabricate Ag₂S nanoworms via microwave irradiation

(100 U mL⁻¹) in a humidified atmosphere with 5% CO₂ at 37 °C. The cells were seeded in 96-well plates at 5×10^3 cells per well in DMEM medium and incubated overnight. The cells were then treated in triplicate with fresh medium containing grade concentrations (0.01, 0.05, 0.20, 1.00 mg mL⁻¹) of the nanoworms and incubated at 37 °C for 24 h. Aliquots of MTT solution (10 μL, 5 mg mL⁻¹) were added to each of the wells for 4 h of incubation. After the medium was removed, 150 μL of DMSO was added to each well. The absorbance of the purple formazan was recorded at 490 nm using an ELISA plate reader. The cytotoxicity results were calculated based on the data of three replicate tests.

Characterization

Field emission scanning electron microscopy (FE-SEM) images were obtained using Hitachi S-4800 field emission electron microscope at an accelerating voltage of 10 kV. X-ray powder diffraction (XRD) measurements were performed on a Japan Shimadzu XRD-6000 diffractometer with Cu-K α radiation ($\lambda = 0.15418$ nm); A scanning rate of 0.05 deg s⁻¹ was applied to record the patterns in the 2θ range of 20–70°. Transmission electron microscopy (TEM) images were taken using a JEOL JEM-2100 transmission electron microscope at an accelerating voltage of 200 kV, equipped with selected area electron diffraction (SAED) and X-ray energy dispersive spectroscopy (EDS). The Fourier transform infrared (FTIR) spectra were recorded on a Nicolet 6700 FTIR spectrograph in the wavenumber range of 4000–400 cm⁻¹.

Results and discussion

The synthesis of silver sulfide nanoworms was performed by a two-step procedure. The first step

was the generation of the Ag₂S crystal nuclei by adding TAA into silver (I)–BSA complex solution. Then, Ag₂S nuclei underwent growth or further reactions to form the nanoworm structures under microwave irradiation, as illustrated in Scheme 1. When Na₂S was substituted for TAA, only irregular particles were formed, indicating that the slow release of sulfide ions from TAA was essential for the formation of the nanoworms.

The morphology and dimensions of the product were determined by SEM. As shown in Fig. 1a, the product presents a worm-like morphology with nanometer-sized diameters. The crystal structure and crystallinity were examined by XRD. In Fig. 1b, the nanoworms exhibit good crystal quality; all of the reflections can be indexed to monoclinic acanthite, confirming good agreement with the reported data for α -Ag₂S (JCPDS Card File: 14-0072) after considering Scherrer broadening (Wang and Qi 2008).

Detailed structural information of the nanoworms was obtained by TEM. Figure 2a is a representative TEM image of the Ag₂S nanoworms obtained from the typical experiment. The nanoworm is composed of several adjacent nanoparticles attached with connective interfaces. It has the sizes of about 50 nm in diameter and hundreds of nanometers in length. The SAED pattern in Fig. 2b reveals that the nanoworm is crystalline, and adopts a monoclinic acanthite structure. Its EDS spectra in Fig. 2c show the significant presence of Ag and S, besides the peaks for Cu and C, which arise from the supporting grid of Cu and covering film of C in the sample preparation, respectively. Based on the relative area under the peaks for Ag and S, the atomic ratio of Ag to S is evaluated to be approx. 2:1, being in good agreement with the stoichiometric molar ratio of silver sulfide. As shown in Fig. 2d, the center sections of the nanoworms were partly damaged and emptied during long-time TEM observations, since silver sulfide is

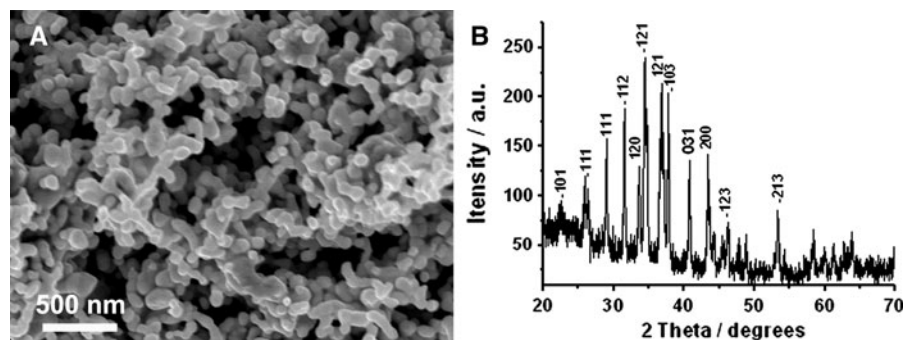
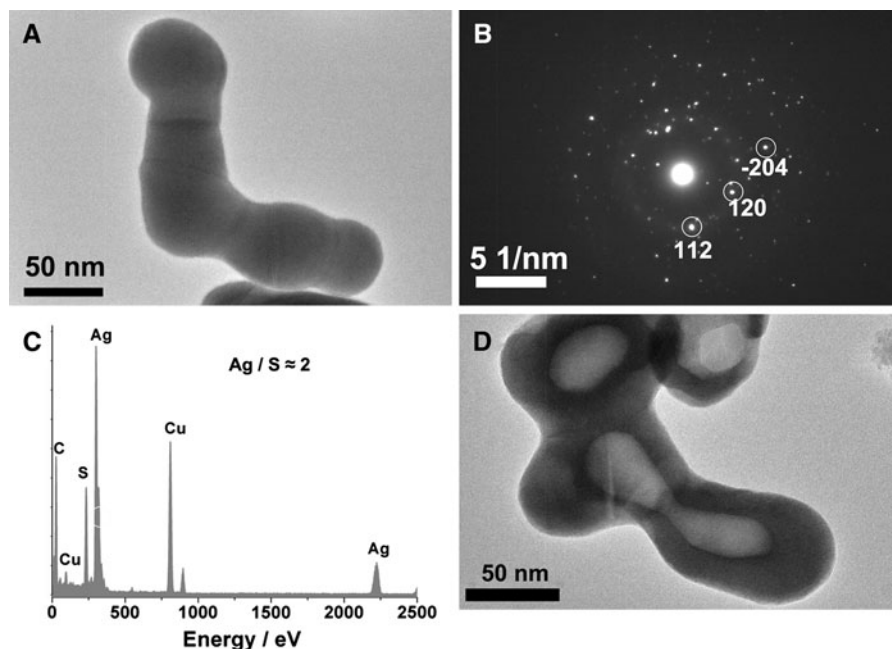


Fig. 1 SEM image (a) and XRD pattern (b) of the as-prepared Ag_2S nanoworms

Fig. 2 Low-magnification TEM image (a), SAED pattern (b), and EDS spectra (c) of the as-prepared Ag_2S nanoworms; and low-magnification TEM image of the damaged nanoworms due to the long-time electronbeam irradiation (d)



easy to decompose under the intense electronbeam irradiation (Xu et al. 2010). The edges of the nanoworm look fuzzy and amorphous, which was presumed to be the BSA coating (Yang et al. 2006). By setting a control experiment, silver sulfide was prepared in the aqueous solution without BSA, in which the Ag_2S crystals were badly aggregated with different sizes. The results show that BSA plays a key role in controlling and regulating the attachment of Ag_2S nanoparticles into the nanoworms. These observations show the nanoworms were assembled by multiple adjacent Ag_2S nanoparticles and stabilized by a layer of BSA attached to their surface. The TEM result is consistent with that obtained from the SEM observation.

The involvement of BSA in the nanoworms was further studied by FTIR spectroscopy. As seen in Fig. 3, the IR peaks of pure BSA at 3410, 1640, and 1521 cm^{-1} are assigned to the stretching vibration of $-\text{OH}$ groups, amide I, and amide II bands, respectively. In comparison, the nanoworms show the similar typical absorptions with BSA molecules with negligible variations. These evidences confirm the existence of BSA in the nanoworms.

High-resolution TEM was used to obtain further insights into the crystal state of the nanoworms. A close look to their connection sections was performed, and their correlative FFT patterns were extracted to obtain some crystallographic information. As shown in Fig. 4a, more nanoworm

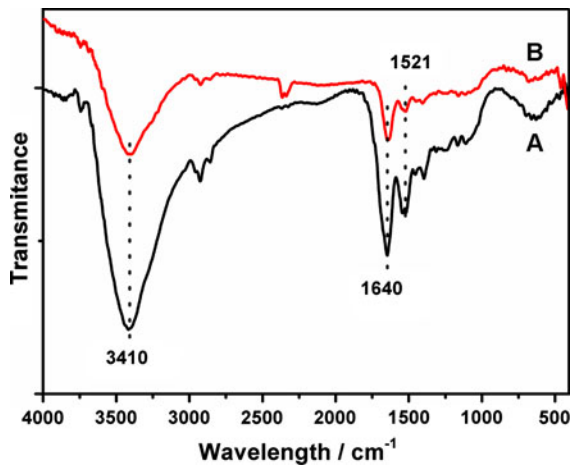


Fig. 3 The FTIR spectra of pure BSA (A) and BSA–Ag₂S nanoworms (B)

assemblies are clearly observed, which were formed by the attachment of multiple nanoparticles as building blocks (Banfield et al. 2000; Yang et al. 2008). In Fig. 4b, the two adjacent nanoparticles exhibit clear lattice fringes; both of the FFT patterns from the frames #1 and #2 present the (–112) planes of monoclinic acanthite with the difference in crystallographic orientation, and the angles between the two crystal planes was 73°. In Fig. 4c, the FFT

patterns of the adjacent nanoparticles from the frames #1 and #2 exhibit, respectively, the (–112) and (112) planes of monoclinic acanthite with different crystallographic orientations and the angle between the two crystal planes were 69°. In Fig. 4d, the FFT analyses of the two adjacent nanoparticles from the frames #1 and #2 exhibit the (120) planes of monoclinic acanthite with different crystallographic orientations and the angle between the two crystal planes was 45°. These results indicate that these adjacent nanoparticles did not share the same crystallographic orientation, although they might possibly have the same crystallographically specific surfaces. That is, the nanoworms are formed when misorientation of the adjacent nanoparticles happens at the interfaces under microwave irradiation (Penn and Banfield 1998). They were expected to rotate and fuse each other to reach the thermodynamically favorable interface configuration if free growing at ambient temperature was allowed instead of microwave irradiation as indicated in the literature (Yang et al. 2006, 2008). This is possibly because the kinetic barrier under microwave irradiation is too high to bring the rotation and fusion transition about, and thus cause the formation of the nanoworms (Chen et al. 1997).

The time-dependent shape evolution of Ag₂S nanoworms was studied to keep track of the

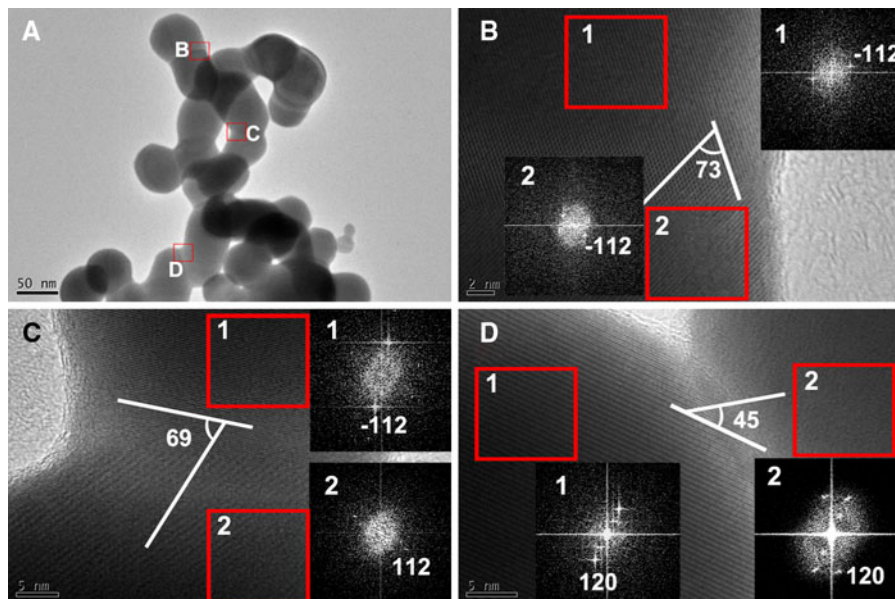


Fig. 4 Low-magnification TEM image of the nanoworms (a), and high-resolution TEM images of the framed area marked in a (b–d). Inset: FFT patterns of the frames #1 and #2 in each high-resolution TEM image, displaying the growth orientation of nanocrystals

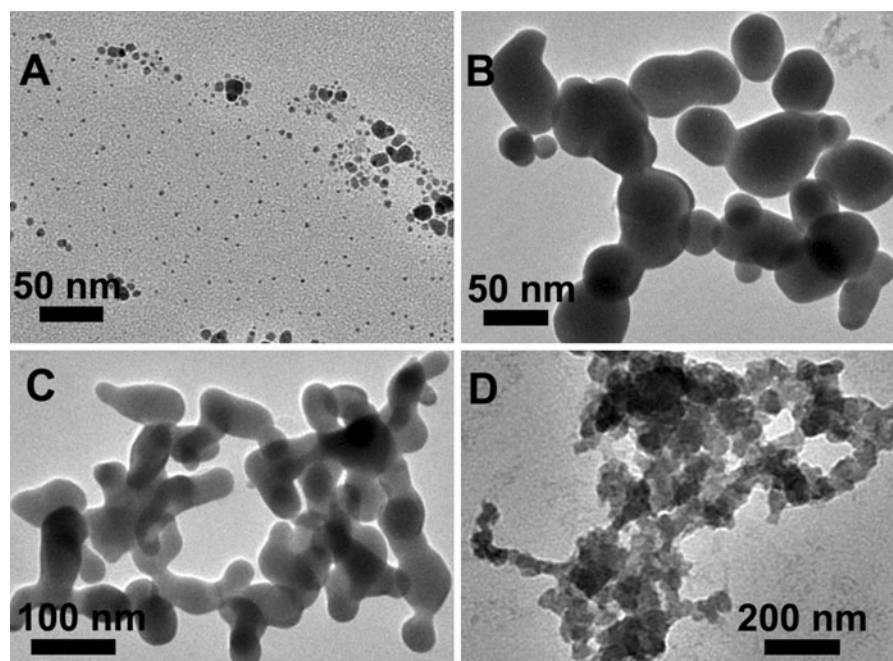


Fig. 5 TEM images of the Ag_2S nanoworms obtained at different time intervals: 5 min (a), 15 min (b), 30 min (c), and 80 min (d), respectively

nanoworm growth. Figure 5 presents the typical morphology of the nanoworms for different treatment times. After 5 min of microwave hydrothermal treatment, the obtained sample was mainly composed of scattered nanoparticles with diameters in the range of 5–20 nm (Fig. 5a). For a heating time of 15 min, the nanoparticles grew larger, and several adjacent nanoparticles became attached (Fig. 5b). When heated for 30 min, these nanoworms had a wide range in length, and all the nanoparticles disappeared (Fig. 5c). If the heating time was increased to 50 min, these nanoworms grew longer with more nanoparticles attached with the connective interfaces (Fig. 4a). To investigate further, the heating time was even prolonged to 80 min, and it was found, however, that the nanoworms seem interlaced and aggregated (Fig. 5d). According to the above phenomena and high-resolution TEM analyses, it could be presumed that the nanoworms were formed by the misorientation attachment of multiple adjacent nanoparticles at the connective interfaces under appropriate microwave irradiation. The nanoworms are expected to be attractive and promising building blocks for advanced materials and devices.

To examine the feasibility of the nanoworms in biorelated fields, the cytotoxicity was tested on the human cervical cancer cell line HeLa by MTT assay. Figure 6 shows the cellular viability of HeLa cells treated with the grade concentrations of the nanoworms after 24 h. The viability of untreated cells in the blank group was assumed to be 100%. When the concentration is lower than 0.05 mg mL^{-1} , the nanoworms exhibit a negligible cytotoxic profile compared with the blank group. When the concentrations are increased to 0.2 and 1.0 mg mL^{-1} , over 100% of the cellular viability is observed. These results indicate that the nanoworms barely exhibit cytotoxicity, and even contribute to cell proliferation with increasing concentration. The proliferation effect of the nanoworms may stem from the involvement of BSA since the protein BSA is a nutriment for many cells (Xing et al. 2009a). Thus, the biocompatibility of the nanoworms is greatly enhanced. This study provides a new insight into the preparation of protein-modified nanocrystals with excellent biocompatibility, which present bioactive functionalities throughout the nanocrystal surface for further biological interactions or couplings and then be used in

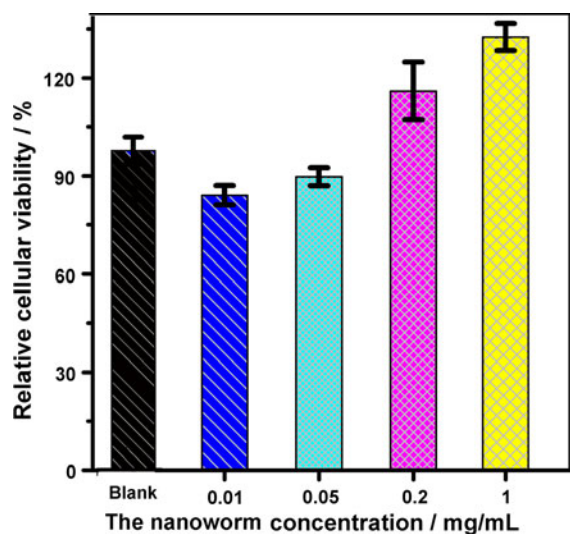


Fig. 6 Cytotoxicity of different concentrations of the nanoworms against human cervical cancer cell line HeLa after 24 h with untreated cells as a negative reference

life sciences for luminescence tagging, drug delivery, and many other aspects (Reches and Gazit 2003).

Conclusions

In summary, a rapid synthetic route based on microwave-assisted hydrothermal reaction has been developed to prepare the biocompatible silver sulfide nanoworms by reacting silver nitrate and TAA in the BSA aqueous solution. The nanoworms were assembled by the misoriented attachment of multiple adjacent Ag_2S nanoparticles and stabilized by a layer of BSA. These results could benefit the general understanding of crystal growth mechanisms and the preparation of highly controlled nanostructures. The BSA coating ensures that the nanoworms are biocompatible and easy to fabricate and process further into more complex structures. Furthermore, this study provided a new insight into the preparation of the protein-modified nanocrystals, which would have great potential not only in biorelated fields, but also in advanced microdevices.

Acknowledgments The authors are grateful to the Foundation of State Key Laboratory of Coordination Chemistry of China (No. 2010-20), and the Educational Commission of Henan Province of China (2011A150005) for their financial support.

References

- Banfield JF, Welch SA, Zhang H, Ebert TT, Penn RL (2000) Aggregation-based crystal growth and microstructure development in natural iron oxyhydroxide biomineralization products. *Science* 289:751–754
- Baruwati B, Polshettiwar V, Varma RS (2009) Glutathione promoted expeditious green synthesis of silver nanoparticles in water using microwaves. *Green Chem* 11:926–930
- Brelle MC, Zhang JZ, Nguyen L, Mehra RK (1999) Synthesis and ultrafast study of cysteine- and glutathione-capped Ag_2S semiconductor colloidal nanoparticles. *J Phys Chem A* 103:10194–10201
- Chen C–C, Herhold AB, Johnson CS, Alivisatos AP (1997) Size dependence of structural metastability in semiconductor nanocrystals. *Science* 276:398–401
- Choi SH, An K, Kim EG, Yu JH, Kim JH, Hyeon T (2009) Simple and generalized synthesis of semiconducting metal sulfide nanocrystals. *Adv Funct Mater* 19:1645–1649
- Du YP, Xu B, Fu T, Cai M, Li F, Zhang Y, Wang QB (2010) Near-infrared photoluminescent Ag_2S quantum dots from a single source precursor. *J Am Chem Soc* 132:1470–1471
- Jang K, Kim SY, Park KH, Jang E, Jun S, Son SU (2007) Shape-controlled synthesis of silver sulfide nanocrystals by understanding the origin of mixed-shape evolution. *Chem Commun* 4474–4476
- Liao ZM, Hou C, Zhao Q, Wang DS, Li YD, Yu DP (2009) Resistive switching and metallic-filament formation in Ag_2S nanowire transistors. *Small* 5:2377–2381
- Lim WP, Zhang Z, Low HY, Chin WS (2004) Preparation of Ag_2S nanocrystals of predictable shape and size. *Angew Chem Int Ed* 43:5685–5689
- Liu SH, Qian XF, Yin J, Hong L, Wang XL, Zhu ZK (2002) Synthesis and characterization of Ag_2S nanocrystals in hyperbranched polyurethane at room temperature. *J Solid State Chem* 168:259–262
- Liu ZP, Liang JB, Xu D, Lu J, Qian YT (2004) A facile chemical route to semiconductor metal sulfide nanocrystal superlattices. *Chem Commun* 2724–2725
- Liu SH, Lu F, Zhu JJ (2011a) Highly fluorescent Ag nanoclusters: microwave-assisted green synthesis and Cr^{3+} sensing. *Chem Commun* 47:2661–2663
- Liu SH, Lu F, Jia X, Cheng F, Jiang L, Zhu JJ (2011b) Microwave-assisted synthesis of a biocompatible polyacid-conjugated Fe_3O_4 superparamagnetic hybrid. *Cryst-EngComm* 13:2425–2429
- Lu QY, Gao F, Zhao DY (2002) Creation of a unique self-supported pattern of radially aligned semiconductor Ag_2S nanorods. *Angew Chem Int Ed* 41:1932–1934
- Mamedova NN, Kotov NA, Rogach AL, Studer J (2001) Albumin–CdTe nanoparticle bioconjugates: preparation, structure, and interunit energy transfer with antenna effect. *Nano Lett* 1:281–286
- Mao CJ, Geng J, Wu XC, Zhu JJ (2010) Selective synthesis and luminescence properties of self-assembled SrMoO_4 superstructures via a facile sonochemical route. *J Phys Chem C* 114:1982–1988
- Niu X, Liu S, Xing R, Wang X, Zhang B, Chen J, Yang L (2007) Synthesis of single-crystalline silver sulfide

- nanowires by diffusion in porous anodic aluminium oxide template. *Mater Lett* 61:5098–5101
- Pal A, Shah S, Devi S (2009) Microwave-assisted synthesis of silver nanoparticles using ethanol as a reducing agent. *Mater Chem Phys* 114:530–532
- Pan HC, Tao XC, Mao CJ, Zhu JJ, Liang FP (2007) Aminopolycarboxyl-modified Ag_2S nanoparticles: synthesis, characterization and resonance light scattering sensing for bovine serum albumin. *Talanta* 71:276–281
- Pastoriza-Santos I, Liz-Marzán LM (2002) Formation of PVP-protected metal nanoparticles in DMF. *Langmuir* 18:2888–2894
- Penn RL, Banfield JF (1998) Imperfect oriented attachment: dislocation generation in defect-free nanocrystals. *Science* 281:969–971
- Qin DZ, Ma XM, Yang L, Zhang L, Ma ZJ, Zhang J (2008) Biomimetic synthesis of HgS nanoparticles in the bovine serum albumin solution. *J Nanopart Res* 10:559–566
- Reches M, Gazit E (2003) Casting metal nanowires within discrete self-assembled peptide nanotubes. *Science* 300:625–627
- Sadtler B, Demchenko DO, Zheng H et al (2009) Selective facet reactivity during cation exchange in cadmium sulfide nanorods. *J Am Chem Soc* 131:5285–5293
- Song Q, Ai X, Topuria T et al (2010) Microwave-assisted synthesis of monodispersed CdTe nanocrystals. *Chem Commun* 46:4971–4973
- Teranishi T, Saruyama M, Kanehara M (2009) Seed-mediated synthesis of metal sulfide patchy nanoparticles. *Nanoscale* 1:225–228
- Wang HL, Qi LM (2008) Controlled synthesis of Ag_2S , Ag_2Se , and Ag nanofibers using a general sacrificial template and their application in electronic device fabrication. *Adv Funct Mater* 18:1249–1256
- Wang DS, Xie T, Peng Q, Li YD (2008) Ag , Ag_2S , and Ag_2Se nanocrystals: synthesis, assembly, and construction of mesoporous structures. *J Am Chem Soc* 130:4016–4022
- Wang DS, Zheng W, Hao CH, Peng Q, Li YD (2009) A synthetic method for transition-metal chalcogenide nanocrystals. *Chem Eur J* 15:1870–1875
- Wu CC, Shiau CY, Ayele DW, Su WN, Cheng MY, Chiu CY, Hwang BJ (2010) Rapid microwave-enhanced solvothermal process for synthesis of CuInSe_2 particles and its morphologic manipulation. *Chem Mater* 22:4185–4190
- Xing RM, Wang XY, Yan LL, Zhang CL, Yang Z, Wang XH, Guo ZJ (2009a) Fabrication of water soluble and biocompatible CdSe nanoparticles in apoferritin with the aid of EDTA. *Dalton Trans* 1710–1713
- Xing RM, Wang XY, Zhang CL, Zhang YM, Wang Q, Yang Z, Guo ZJ (2009b) Characterization and cellular uptake of platinum anticancer drugs encapsulated in apoferritin. *J Inorg Biochem* 103:1039–1044
- Xu Z, Bando Y, Wang WL, Bai XD, Golberg D (2010) Real-time in situ HRTEM-resolved resistance switching of Ag_2S nanoscale ionic conductor. *ACS Nano* 4:2515–2522
- Yang L, Xing RM, Shen QM, Jiang K, Ye F, Wang JY, Ren QS (2006) Fabrication of protein-conjugated silver sulfide nanorods in the bovine serum albumin solution. *J Phys Chem B* 110:10534–10539
- Yang L, Yang HY, Yang ZX, Cao YX, Ma XM, Lu ZS, Zheng Z (2008) Observation of rotated-oriented attachment during the growth of Ag_2S nanorods under mediation of protein. *J Phys Chem B* 112:9795–9801
- Yang L, Liu SH, Zhang BF, Xing RM, Wang HJ, Zhou JG (2010) The synthesis and crystallization mechanism of protein-conjugated silver sulfide nanowires with hierarchical structure. *Mater Lett* 64:1598–1600
- Zhang WX, Zhang L, Hui ZH, Zhang XM, Qian YT (2000) Synthesis of nanocrystalline Ag_2S in aqueous solution. *Solid State Ion* 130:111–114
- Zhu J, Palchik O, Chen S, Gedanken A (2000) Microwave assisted preparation of CdSe , PbSe , and Cu_{2-x}Se nanoparticles. *J Phys Chem B* 104:7344–7347
- Zhu YJ, Wang WW, Qi RJ, Hu XL (2004) Microwave-assisted synthesis of single-crystalline tellurium nanorods and nanowires in ionic liquids. *Angew Chem Int Ed* 43:1410–1414